Olena GUMEN
National University of Ukraine "Kyiv Polytechnic Institute"
Viktor MILEIKOVSKYI, Volodymyr DZIUBENKO
Kyiv National University of Construction and Architecture

JUSTIFICATION OF DUCT SHAPE BETWEEN TWO WELDED FILMS OF A FILM ECONOMIZER FOR DEEP HEAT UTILIZATION

We justificate a shape of a duct between two welded film sheets in economizer, developed at the Heat Gas Supply and Ventilation Department of Kyiv National University of Construction and Architecture by PhD. Eugen Kezlia. Analytically proved that idealized section of the channel is digonal. It is formed by two arcs of the same radius. We offer an algorithm for approximating an experimental duct shape that provides equal section area, perimeter, and equivalent diameter.

Keywords: polymer heat exchanger, digonal duct, section approximation

INTRODUCTION

Heat recovery of exhaust air, combustion materials, technological waste, etc. is a topical trend of energy efficiency. Today many different economizer constructions are developed for different purposes [1-12]. To decrease price, metal consumption and to eliminate corrosion developers use non-metal materials [13, 14]. For low-potential waste energy one of the best economizers [15, 16] by cost-efficiency was developed at Heat Gas Supply and Ventilation Department of Kyiv National University of Construction and Architecture by Ph.D. Yevgen Kezlia (Fig. 1a, b). Each section of the device is made from two welded polymer films.

The shape of the duct was investigated experimentally by casts (Fig. 1b, c). It was interpolated by two circle arcs (Fig. 1d). Each arc is based on two welding points and the point of maximum distance between the sheets. This form of channel called digonal as the same figure in the spherical geometry. The area accuracy was 6%. For current high requirements of energy efficiency this accuracy is not enough. So we need to offer refined approximation of the duct shape.

1. ANALYTICAL DETERMINATION OF THE DUCT SECTION SHAPE

To clarify the ducts shape we perform its analytical calculation. Let us assume constant pressure difference Δp between the heat carrier in a duct section and in the device space. It is so large that bending forces in the films are not essential.

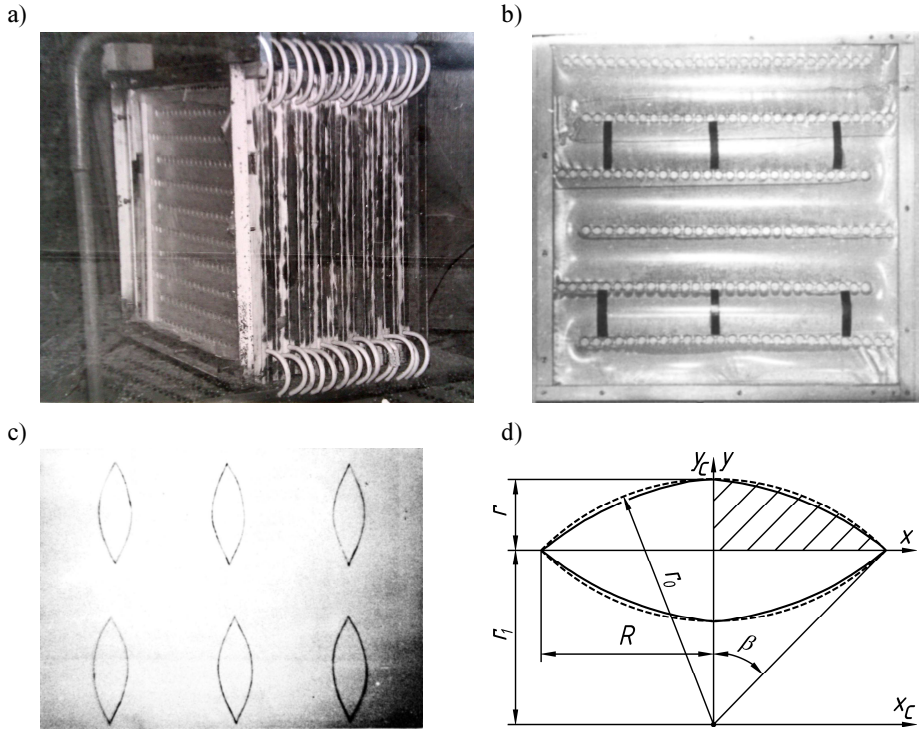

Fig. 1. Heat exchanger, developed by E. Kezlia: a) the heat exchanger, b) one section with casts, c) the casts shape, d) the cast shape interpolation: solid line - experimental shape, dashed line - interpolated shape

We introduce the Euclidean coordinate system (x, y), which is tied to the section centre (Fig. 2a). We consider an arbitrary section of the homogeneous films under normal pressure forces. Two points of the section are fixed: ($-R$, 0) and (R, 0). R is the length of the section long axis half.

We select an element of the film at the section with length Δs. At both ends of the element there are two tension forces $T(x)$ and $T(x + \Delta x)$. The element has normal pressure force P per one length unit of the deepness. Its projections P_x and P_y on the x and y-axis is the product of the pressure difference Δp and the length Δy and Δx of the element projection to the normal axis.

The equilibrium equations of the selected item:

$$\begin{aligned} T(x+\Delta x)\cos(\alpha(x+\Delta x)) - T(x)\cos(\alpha(x)) &= P_x = \pm \Delta p\, \Delta y \\ T(x+\Delta x)\sin(\alpha(x+\Delta x)) - T(x)\sin(\alpha(x)) &= P_y = \pm \Delta p\, \Delta x \end{aligned} \quad (1)$$

The signs in the equations (1) are independent and correspond to different branches of the curve in each quadrant. If the length Δs of the element approaches zero, the equations (1) take the following differential form:

$$d\big(T(x)\cos(\alpha(x))\big) = \pm \Delta p\, dy;\ \ \mathrm{d}\big(T(x)\sin(\alpha(x))\big) = \pm \Delta \mathrm{p}\, \mathrm{d}x \quad (2)$$

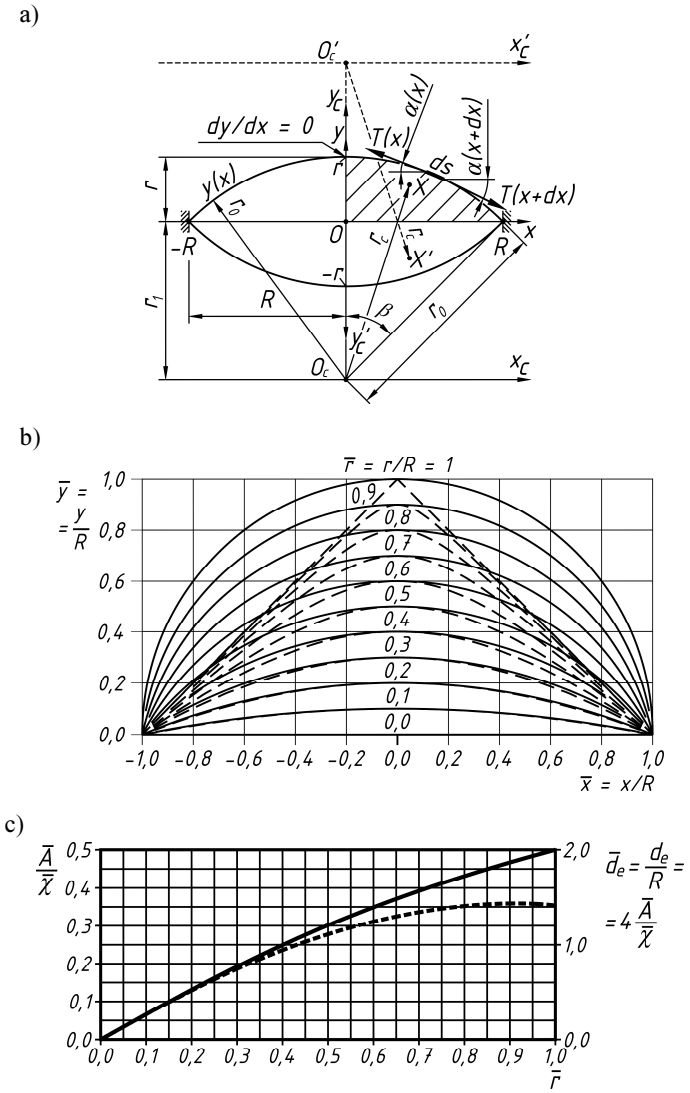

Fig. 2. Theoretical ducts shape: a) scheme, b) solution of the differential equations, c) relative area per perimeter and equivalent diameter: solid line - digonal solution, dashed line - hyperbolic solution

In the equations (2) we replace sine and cosine by tangent - the first derivative. We carry out basic transformation and integration with constants c_0, c_1 and c_2:

$$y = c_1 \pm \left|x^2 + c_2 x + c_0\right|^{1/2}, \quad \frac{dy}{dx} = \pm \mathrm{sgn}\left(x^2 + c_2 x + c_0\right) \frac{2x + c_2}{2\left|x^2 + c_2 x + c_0\right|^{1/2}} \tag{3}$$

To find appropriate solutions of the equations (2) we may use boundary conditions. Both branches and their conjugation at $x = 0$ must satisfy the conditions of

symmetry and smoothness: at $x = 0$ $dy / dx = 0$. This condition causes $c_2 = 0$ by the equations (3). Fixed points provide the following conditions: at $x = \pm R$, $y = 0$ and at $x = 0$, $y = \pm r$ – length of the short axis half. After elementary transformations there are only two meaningful solutions of the equations (2). First solution (Fig. 2b) is hyperbolic:

$$\bar{y} = \pm\left(\bar{r}_0 - \left(\bar{r}_1^2 + \bar{x}^2 \right)^{1/2} \right) \tag{4}$$

where: $\bar{r}_0$ - shift of the hyperbole centre (not vertex) from the section centre relative to R and $\bar{r}_1$ - length of the hyperbole axes half:

$$\bar{r}_0 = r_0/R = \left(1 + \bar{r}^2\right)/(2\bar{r});\ \bar{r}_1 = r_1 / R = \left(1 - \bar{r}^2\right)/(2\bar{r}) \tag{5}$$

These lengths can not be shown at the Figure 2 a. The section area per perimeter is shown by dashed line on the Figure 2c.

The second solution (Fig. 2 b) is digonal:

$$\bar{y} = \pm\left(\left(r_0^2 - \bar{x}^2 \right)^{1/2} - \bar{r}_1 \right) \tag{6}$$

where: $\bar{r}_0$ - a radius of the digone arcs relative to R and $\bar{r}_1$ - shift of the arc centre from the section centre by the equations (5) shown on the Figure 2a.

Perimeter of the section (6) relative to R:

$$\bar{\chi} = \chi / R = 4\bar{r}_0 \arcsin\left(1/\bar{r}_0\right) \tag{7}$$

Area of the section (6) relative to R^2 using the equation (7):

$$\bar{A} = 2\bar{r}_0^2 \arcsin\left(1/\bar{r}_0\right) - 2\bar{r}_1 = 0.5\bar{r}_0\bar{\chi} - 2\bar{r}_1 \tag{8}$$

By the known formula the equivalent diameter may be calculated using formulas (7) and (8):

$$\bar{d}_e = d_e / R = 4\bar{A}/\bar{\chi} \tag{9}$$

From two solutions (4) and (6) we may choose one that has more area per perimeter (Fig. 2c). This is the digonal section (6). If the ratio of the axes length $\bar{r}_0 = r/R$ approaches 1 the hyperbolic solution (4) degenerates to angle that is physically impossible. So this solution is invalid. The digonal solution (6) degenerates to circle that is true. So we prove the hypothesis of Yevgen Kezlia [15, 16] about the digonal ducts shape.

2. EXPERIMENTAL SECTION APPROXIMATION

The main problem is the approximation of the experimental shape of the duct. The experimental section deviates from theoretical because of bend forces at the

welding and the films softness. The flow velocity and pressure loss at known flow are coincide if the area and perimeter (equivalent diameter (9)) are equal in both duct sections. The heat exchange depends on the duct surface area that is the section perimeter multiplied by the duct length. So the most precise result will be obtained if we approximate the section preserving the area and the perimeter. To do it we must solve the equation system (5), (7) and (8).

To simplify the process we use the dimensionless parameter A/χ^2 (Fig. 3):

$$\frac{A}{\chi^2} = \left(\left(\frac{1+\bar{r}^2}{2\bar{r}}\right)^2 \arcsin\left(\frac{2\bar{r}}{1+\bar{r}^2}\right) - \frac{1-\bar{r}^2}{2\bar{r}}\right) \Big/ \left(8\left(\frac{1+\bar{r}^2}{2\bar{r}}\right)^2 \arcsin^2\left(\frac{2\bar{r}}{1+\bar{r}^2}\right)\right) \quad (10)$$

The solution of the equation (10) for the parameter $\tilde{A} = 4\pi(A/\chi^2)$ with the error no more than 1,03% is:

$$\bar{r} = r/R = \left(1 - \left(1 - \tilde{A}\right)^{0.4746}\right) - 0.0725\tilde{A}^{1.73}\left[1 - \tilde{A}^{44.4}\right] \quad (11)$$

The correction in the square brackets may be eliminated at $A/\chi^2 \le 0.07318$ without the accuracy loss.

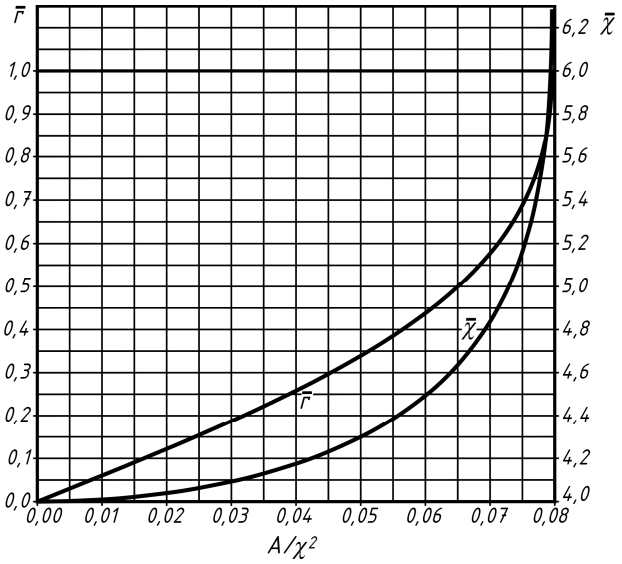

Fig. 3. Radius ratio and perimeter

The algorithm of the approximation is:

1. We measure the perimeter χ and the area A. The easiest way is digitizing, vectoring the image and perform measurements in a drawing program;
2. We calculate the ratio A/χ^2.

3. We calculate the axes length ratio $\bar{r}$ by the equation (11) or Figure 3. If the accuracy is not enough we may solve the equation (10) numerically using previous result as first approximation.
4. According to the equation (7) we determine the relative perimeter $\bar{\chi}$.
5. We determine the length of the radius:

$$R = \chi / \bar{\chi}, r = R\bar{r} \tag{12}$$

Our interpolation of the heat exchanger ducts developed by Yevgen Kezlia gives deviation between interpolated and measured axes length within measurement error (0.25 mm). It provides the best match for the pressure loss and heat transfer coefficient because of the accurate match of the section area and perimeter.

CONCLUSIONS

1. We theoretically prove the digonal shape of the duct between welded polymer films by equilibrium equations of infinitely small film parts.
2. Direct measurement of section axes length using casts do not give sufficient accuracy to determine the area and the equivalent diameter of the duct. We offer an algorithm of approximating the form of casts. It provide more accurate results for pressure loss, velocity of heat carrier and heat exchange.

Acknowledgements

The authors thanks to docent of the Heat Gas Supply and Ventilation Department PhD Mykola Stepanov (1943-2012) who was the scientific adviser of this work until 2012.

REFERENCES

[1] Rudenko O., Mezentseva O., Terekh O., Efficiency of Introduction of Innovation Energy Saving Equipment at Ukrainian Housing and Public Utilities, Business Inform 2014, Iss. 3, pp. 220-224.
[2] Kolodyazhny S., Kavygin A., Design of Modern Plate Recuperators with the Use of Function of Efficiency Coefficient, Vestnik Volgogradskogo Gosudarstvennogo Arhitekturno-Stroitelnogo Universiteta. Seriya : Stroitelstvo i Arhitektura 2014, Iss. 36(55), pp. 182-188.
[3] Karyakina M., Justification of The Mathematical Model of Heat And Moisture Transfer In Heat Recuperators of High Efficiency, Internet-Vestnik VolgGASU 2014, Iss. 1(31).
[4] De Antonellis S., Intini M., Joppolo C., Leone C., Design Optimization of Heat Wheels for Energy Recovery in HVAC Systems, Energies 2014, Vol. 7, Iss. 11, pp. 7348-7367.
[5] Bermúdez-Valencia L., Sarria-López B., Research on Energy Indexes of Cogenerated Plants with Gas Turbines and Heat Recuperator Steam Generators // CT&F - Ciencia, Tecnología y Futuro 2012, Vol. 4, Iss. 5, pp. 85-100.
[6] Kussul E., Makeyev O., Baidyk T., Olvera O., Design of Ericsson Heat Engine with Micro Channel Recuperator, ISRN Renewable Energy 2012, Vol. 2012.
[7] Wnęk M., The Dynamic Characteristics Research of Compact Heat Regenerator used in Regenerative Burners for Metallurgical Heating Furnaces, Archives of Metallurgy and Materials 2014, Vol. 59, Iss. 2, pp. 805-808.

[8] Yang D., Chen L., Ge Y., Sun F., Exergy analyses of an endoreversible closed regenerative Brayton cycle CCHP plant, International Journal of Energy and Environment 2014, Vol. 5, Iss. 6, pp. 655-668.
[9] Pikra G., Purwanto A., Santoso A., Effect of Regenerative Organic Rankine Cycle (RORC) on the Performance of Solar Thermal Power in Yogyakarta, Indonesia, Mechatronics, Electrical Power, and Vehicular Technology 2013, Vol. 4, Iss. 1, pp. 25-32.
[10] Qi X., Guo Q., Analysis of Start-Up Characteristics of a Honeycomb Regenerator, Research Journal of Applied Sciences, Engineering and Technology 2013, Vol. 6, Iss. 20, pp. 3784-3797.
[11] Patel V., Ranpura N.A., Analysis of Regenerator for Reversed Stirling Cycle Which Various Geometry, International Journal of Engineering Sciences & Research Technology 2013, Vol. 2, Iss. 10, pp. 2793-2796.
[12] Patel V., Amitesh P., Dr. Selokar G.R., Priyanka Jhavar, Theoretical Analysis of Regenerator for Reversed Stirling Cycle Review, International Journal of Engineering Sciences & Research Technology 2013, Vol. 2, Iss. 9, pp. 2506-2509.
[13] Grehier A., Rojey A., Échangeurs à condensation en matériau polymère = Condensation Heat Exchangers Made of Polymer Material, Oil & Gas Science and Technology 2006, Vol. 44, Iss. 1, pp. 77-89.
[14] Rocha R.M., Scheffler M., Greil P., Bressiani J.C., Bressiani A.H.A., Obtenção de substratos cerâmicos no sistema Si-Al-O-N-C empregando polissiloxanos e carga de Si e Al2O3 = Ceramic tapes of Si-Al-O-N-C compounds using mixtures of polyssiloxane and Si-Al2O3 fillers, Cerâmica, Vol. 51, Iss. 317, pp. 42-51 (2005).
[15] Росковшенко Ю.К., Середа І.З., Кезля Е.А., Малометальные воздухонагреватели, Строительные материалы, изделия и санитарная техника, Вып. 8., Будивельнык, К.: 1985, с. 85-87.
[16] Степанов М.В., Дзюбенко В.Г. Дідик Л.В., Конвективний теплообмін та теплопередача в полімерному теплообміннику, Будівельні матеріали, вироби та санітарна техніка: науково-технічний збірник., Вип. 23, тов-во Знання України, К.: 2006, с. 112-116.

UZASADNIENIE KSZTAŁT KANAŁU POMIĘDZY DWOMA FILMAMI SPAWANYCH W EKONOMIZERZE FOLIA DO ODZYSKU CIEPŁA GŁĘBOKICH

Mamy uzasadnione kształt kanału pomiędzy dwoma filmami spawanych w wymienniku ciepła, opracowany w dziale dostaw ciepła, gazu i wentylacji Narodowego Uniwersytetu Kijowskiego Budownictwa i Architektury PhD Yevgen Kezlia. Analitycznie udowodnił, że wyidealizowany części Gonal kanału. Jest on utworzony przez dwa łuki o tym samym promieniu. Zaproponowaliśmy algorytm zbliżenia form eksperymentalnych kanału, który zapewnia taką samą powierzchnię przekroju poprzecznego, obwód i średnicę równoważną.

Słowa kluczowe: Polimerowy wymiennik ciepła, Kanał Gonal, przybliżenie przekroju